International Journal of Thermophysics, Vol. 28, No. 1, February 2007 (© 2007)
DOI: 10.1007/s10765-007-0156-4

Mechanical/Thermal Sources in a Micropolar Thermoelastic Medium Possessing Cubic Symmetry without Energy Dissipation

Rajneesh Kumar[1,2] and Praveen Ailawalia[1,3]

Received March 4, 2006

The present problem is concerned with the study of the deformation of a thermoelastic micropolar solid possessing cubic symmetry under the influence of various sources acting on the plane surface. The analytic expressions of displacement components, microrotation, force stress, couple stress, and temperature distribution are obtained in the physical domain for the Green and Nagdhi (G–N) theory of thermoelasticity by applying the integral transforms. A numerical inversion technique has been applied to obtain the solution in the physical domain. The numerical results are presented graphically for a particular material.

KEY WORDS: couple stress; cubic symmetry; integral transform; micropolar thermoelastic; microrotation; thermoelasticity.

1. INTRODUCTION

The classical theory of heat conduction predicts an infinite speed of heat transport, if a material conducting heat is subjected to a thermal disturbance, which contradicts physical facts. Lord and Shulman [1] incorporated a flux rate term into the Fourier's law of heat conduction and formulated a generalized theory giving a finite speed for thermal signals. Green and Lindsay [2] have developed a temperature rate dependent thermoelasticity by including the temperature rate among the constitutive variables which does not violate the classical Fourier's law of heat conduction

[1] Department of Mathematics, Kurukshetra University, Kurukshetra, Haryana 136119, India.
[2] Department of Applied Sciences, RIMT Institute of Engineering and Technology, Dist. Fatehgarh Sahib, Mandi Gobindgarh, Punjab, India.
[3] To whom correspondence should be addressed. E-mail: praveen_2117@rediffmail.com

when the body under consideration has a center of symmetry, and this theory also predicts a finite speed of heat propagation. Green and Naghdi [3] established a new thermomechanical theory of deformable media that uses a general entropy balance. The generalized thermoelasticity theories are supposed to be more realistic than conventional theory in dealing with practical problems involving very large heat fluxes and or short time intervals, like those occurring in laser units and energy channels.

The classical theory of elasticity is inadequate to represent the behavior of some modern engineering structures like polycrystalline materials and materials with fibrous or coarse grain. The study of these materials requires incorporating the theory of oriented media. "Micropolar elasticity" termed by Eringen [4] is used to describe the deformation of elastic media with oriented particles. A micropolar continuum is a collection of interconnected particles in the form of small rigid bodies undergoing both translational and rotational motions. The force at a point of a surface element of bodies of these materials is completely characterized by a stress vector and a couple stress vector at that point.

Following various methods, the elastic fields of various loadings, inclusion and inhomogeneity problems, and interaction energy of point defects and dislocation arrangement have been discussed extensively in the past. Generally all materials have elastic anisotropic properties, which mean that the mechanical behavior of an engineering material is characterized by the direction dependence. However, the three-dimensional study for an anisotropic material is much more complicated to obtain than the isotropic one, due to the large number of elastic constants involved in the calculation. In recent years the elastodynamic response of an anisotropic continuum has received the attention of several researchers. In particular, transversly isotropic and orthotropic materials, which may not be distinguished from each other in plane strain and plane stress, have been more regularly studied. The orthotropic material has the symmetry of its elastic properties with respect to two orthogonal planes, whereas a cubic material is a special case of an orthotropic material that has the same properties along two axes and different properties along the third axis and is invariant to an additional change of coordinates. Kumar and Choudhary [5–7] discussed different types of problems in micropolar orthotropic continua.

A wide class of crystals such as W, Si, Cu, Ni, Fe, Au, Al, etc., which are some frequently used substances, belong to cubic materials. The cubic materials have nine planes of symmetry whose normals are on the three coordinate axes and on the coordinate planes making an angle $\pi/4$ with the coordinate axes. With the chosen coordinate system along the crystalline directions, the mechanical behavior of a cubic crystal can be characterized by three independent elastic constants.

To understand the crystal elasticity of a cubic material, Chung and Buessem [8] presented a convenient method to describe the degree of the elastic anisotropy in a given cubic crystal. Later, Lie and Koehler [9] used a Fourier expansion scheme to calculate the stress fields caused by a unit force in a cubic crystal. Steeds [10] gave a complete discussion on the displacements, stresses, and energy factors of the dislocations for two-dimensional anisotropic materials. Boulanger and Hayes [11] investigated inhomogeneous plane waves in cubic elastic materials. Bertram et al. [12] discussed generation of discrete isotropic orientation distributions for linear elastic cubic crystals. Kobayashi et al. [13] investigated anisotropy and curvature effects for growing crystals. Domanski and Jablonski [14] studied resonances of nonlinear elastic waves in cubic crystals. Destrade [15] considered the explicit secular equation for surface acoustic waves in monoclinic elastic crystals. Zhou and Ogawa [16] investigated elastic solutions for a solid rotating disk with cubic anisotropy. Minagawa et al. [17] discussed the propagation of plane harmonic waves in a cubic micropolar medium. Kumar and Rani [18] studied time harmonic sources in a thermally conducting cubic crystal. Recently, Kumar and Ailawalia [19,20] discussed source problems in micropolar cubic crystals. However, no attempt has been made to study source problems in a micropolar thermoelastic medium possessing cubic symmetry.

The present investigation is to determine the components of displacement, microrotation, and stresses in a micropolar thermoelastic medium possessing cubic symmetry without energy dissipation due to mechanical/thermal sources. The solution is obtained by introducing potential functions after employing an integral transformation technique. The integral transforms are inverted using a numerical method.

2. PROBLEM FORMULATION

We consider a homogeneous, thermoelastic micropolar half-space possessing cubic symmetry. A rectangular coordinate system (x, y, z) having the origin on the surface $y = 0$ and y-axis pointing vertically into the medium is considered. A normal force/thermal source is assumed to be acting at the plane surface $y = 0$ of the rectangular Cartesian co-ordinates. If we restrict our analysis to a plane strain parallel to the xy-plane with a displacement vector $\vec{u} = (u_1, u_2, 0)$ and microrotation vector $\vec{\phi} = (0, 0, \phi_3)$, then the field equations and constitutive relations for a thermoelastic micropolar solid possessing cubic symmetry without energy dissipation in the absence of body forces, body couples, and heat sources can be written by following the equations given by Minagawa et al. [17] and Green and

Naghdi [3] as

$$A_1 \frac{\partial^2 u_1}{\partial x^2} + A_3 \frac{\partial^2 u_1}{\partial y^2} + (A_2 + A_4) \frac{\partial^2 u_2}{\partial x \partial y} + (A_3 - A_4) \frac{\partial \phi_3}{\partial y} - \nu \frac{\partial T}{\partial x} = \rho \frac{\partial^2 u_1}{\partial t^2}, \tag{1}$$

$$A_3 \frac{\partial^2 u_2}{\partial x^2} + A_1 \frac{\partial^2 u_2}{\partial y^2} + (A_2 + A_4) \frac{\partial^2 u_1}{\partial x \partial y} - (A_3 - A_4) \frac{\partial \phi_3}{\partial x} - \nu \frac{\partial T}{\partial y} = \rho \frac{\partial^2 u_2}{\partial t^2}, \tag{2}$$

$$B_3 \nabla^2 \phi_3 + (A_3 - A_4) \left(\frac{\partial u_2}{\partial x} - \frac{\partial u_1}{\partial y} \right) - 2 (A_3 - A_4) \phi_3 = \rho j \frac{\partial^2 \phi_3}{\partial t^2}, \tag{3}$$

$$K^* \nabla^2 T = \rho C^* \frac{\partial^2 T}{\partial t^2} + \nu T_0 \frac{\partial^2}{\partial t^2} \left(\frac{\partial u_1}{\partial x} + \frac{\partial u_2}{\partial y} \right), \tag{4}$$

$$t_{22} = A_2 \frac{\partial u_1}{\partial x} + A_1 \frac{\partial u_2}{\partial y} - \nu T, \tag{5}$$

$$t_{21} = A_4 \left(\frac{\partial u_2}{\partial x} - \phi_3 \right) + A_3 \left(\frac{\partial u_1}{\partial y} + \phi_3 \right), \tag{6}$$

$$m_{23} = B_3 \frac{\partial \phi_3}{\partial y}. \tag{7}$$

where t_{22}, t_{21}, m_{23} are the components of the normal force stress, the tangential force stress, and the tangential couple stress, respectively. A_1, A_2, A_3, A_4, B_3 are characteristic constants of the material such that $A_1 = A_2 + A_3 + A_4, \nu = (A_1 + 2A_2)\alpha_T$, α_T is the coefficient of linear expansion, ρ is the density, j is the microinertia, $K^* = \frac{C^*(A_2+2A_4)}{4}$ is the material constant characteristic of the theory, C^* is the specific heat at constant strain, and $\nabla^2 = \frac{\partial^2}{\partial x^2} + \frac{\partial^2}{\partial y^2}$.

Introducing dimensionless variables defined by

$$x' = \frac{x}{l}, \quad y' = \frac{y}{l}, \quad \phi_3' = \frac{\rho c_1^2}{\nu T_0} \phi_3, \qquad \left\{ t_{22}', t_{21}' \right\} = \frac{\{t_{22}, t_{21}\}}{\nu T_0}, \quad u_1' = \frac{\rho c_1^2}{l \nu T_0} u_1,$$

$$u_2' = \frac{\rho c_1^2}{l \nu T_0} u_2, \quad m_{23}' = \frac{1}{l \nu T_0} m_{23}, \quad T' = \frac{T}{T_0}, \quad h' = lh, \quad t' = \frac{c_1}{l} t,$$
$$a' = \frac{a}{l}, \quad F' = \frac{F}{\nu T_0}. \tag{8}$$

where l is a standard length and $c_1^2 = \frac{A_1}{\rho}$, in Eqs. (1)–(4) and introducing potential functions defined by

$$u_1 = \frac{\partial q}{\partial x} + \frac{\partial \Psi}{\partial y}, \quad u_2 = \frac{\partial q}{\partial y} - \frac{\partial \Psi}{\partial x}, \tag{9}$$

in the resulting dimensionless equations, where $q\,(x, y, t)$ *and* $\Psi\,(x, y, t)$ are scalar potential functions, we obtain

$$\left[\frac{\partial^2}{\partial x^2} + \frac{\partial^2}{\partial y^2} - \frac{\partial^2}{\partial t^2}\right] q - T = 0, \tag{10}$$

$$\left[a_{12}\frac{\partial^2}{\partial x^2} + a_{13}\frac{\partial^2}{\partial y^2} - \frac{\partial^2}{\partial t^2}\right] \Psi + a_{14}\phi_3 = 0, \tag{11}$$

$$a_{15}\nabla^2\Psi + \left[\nabla^2 + 2a_{15} - a_{16}\frac{\partial^2}{\partial t^2}\right]\phi_3 = 0, \tag{12}$$

$$\varepsilon\frac{\partial^2}{\partial t^2}\nabla^2 q + \left[a_{17}\frac{\partial^2}{\partial t^2} - \nabla^2\right] T = 0, \tag{13}$$

where

$$a_{12} = 1 - \frac{(A_2 + A_4)}{\rho c_1^2}, \quad a_{13} = \frac{A_3}{\rho c_1^2}, \quad a_{14} = \frac{A_3 - A_4}{\rho c_1^2},$$
$$a_{15} = \frac{(A_4 - A_3)\, l^2}{B_3}, \quad a_{16} = \frac{\rho j c_1^2}{B_3}, \quad a_{17} = \frac{\rho C^* c_1^2}{K^*}, \quad \varepsilon = \frac{\nu^2 T_0}{\rho \omega K^*}. \tag{14}$$

Applying the Laplace transform with respect to time 't' defined by

$$\left\{\overline{q}, \overline{\Psi}, \overline{T}, \overline{\phi}_3\right\}(x, y, p) = \int_0^\infty \{q, \Psi, T, \phi_3\}(x, y, t)\, e^{-pt}\, dt, \tag{15}$$

and then the Fourier transform with respect to 'x' defined by

$$\left\{\tilde{q},\ \tilde{\Psi},\ \tilde{T},\tilde{\phi}_3\right\}(\xi,y,p)=\int_{-\infty}^{\infty}\left\{\overline{q},\ \overline{\Psi},\ \overline{T},\overline{\phi}_3\right\}(x,y,p)\,e^{i\xi x}\,dx, \tag{16}$$

on Eqs. (10)–(13) and eliminating $\tilde{T}$ and $\tilde{\phi}_3$ from the resulting expressions we get

$$\left[\frac{d^4}{dy^4}+A^*\frac{d^2}{dy^2}+B^*\right]\tilde{q}=0, \tag{17}$$

$$\left[\frac{d^4}{dy^4}+C^*\frac{d^2}{dy^2}+D^*\right]\tilde{\Psi}=0, \tag{18}$$

where

$$\begin{aligned}
A^* &= -\left[a_{17}p^2+2\xi^2+(1+\varepsilon)\,p^2\right],\\
B^* &= \left[\left(\xi^2+p^2\right)\left(a_{17}p^2+\xi^2\right)+\varepsilon p^2\xi^2\right],\\
C^* &= -\left[\left(\xi^2+a_{16}p^2-2a_{15}\right)+\frac{1}{a_{13}}\left(a_{12}\xi^2+p^2\right)+\frac{a_{14}a_{15}}{a_{13}}\right],\\
D^* &= \frac{1}{a_{13}}\left[\left(a_{12}\xi^2+p^2\right)\left(\xi^2+a_{16}p^2-2a_{15}\right)+a_{14}a_{15}\xi^2\right].
\end{aligned} \tag{19}$$

The roots of Eqs. (17) and (18) are given by

$$q_{1,2}^2=\frac{-A^*\pm\sqrt{A^{*2}-4B^*}}{2},\quad q_{3,4}^2=\frac{-C^*\pm\sqrt{C^{*2}-4D^*}}{2}. \tag{20}$$

The solutions of Eqs. (17) and (18) satisfying the radiation conditions are given by

$$\tilde{q} = D_1\exp(-q_1y)+D_2\exp(-q_2y), \tag{21}$$
$$\tilde{\Psi} = D_3\exp(-q_3y)+D_4\exp(-q_4y), \tag{22}$$
$$\tilde{T} = a_1^*D_1\exp(-q_1y)+a_2^*D_2\exp(-q_2y), \tag{23}$$
$$\tilde{\phi}_3 = a_3^*D_3\exp(-q_3y)+a_4^*D_4\exp(-q_4y), \tag{24}$$

where

$$a_n^*=q_n^2-\left(\xi^2+p^2\right),\quad a_\Theta^*=\frac{1}{a_{14}}\left(a_{12}\xi^2+p^2-a_{13}q_\Theta^2\right),\quad n=1,2;\ \Theta=3,4. \tag{25}$$

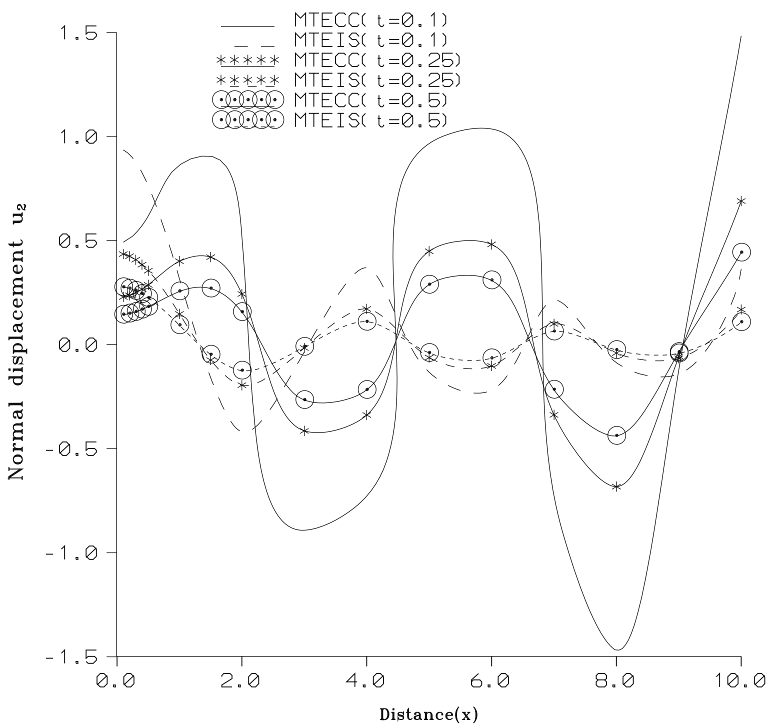

Fig. 1. Variation of normal displacement u_2 with distance x (concentrated normal force: insulated boundary).

3. BOUNDARY CONDITIONS

3.1. Mechanical Source on the Surface of Half-space

The boundary conditions on the surface $y=0$ are

$$t_{22}=-F\psi_1(x)\,\delta(t), \quad t_{21}=0, \quad m_{23}=0, \quad \frac{\partial T}{\partial y}+hT=0. \tag{26}$$

where $\delta(t)$is the Dirac delta function, $\psi_1(x)$ specifies the vertical traction distribution function along the x-axis, F is the magnitude of the applied force, and h is the heat transfer coefficient where $h\to\infty$ for an isothermal boundary and $h\to 0$ for an insulated boundary.

Applying Laplace and Fourier transforms defined by Eqs. (15) and (16) on the boundary conditions Eq. (26) and using Eqs. (5)–(9) and (21)–(24), we get the expressions for displacement components, microrotation, force stress, couple stress, and temperature distribution for a thermoelastic

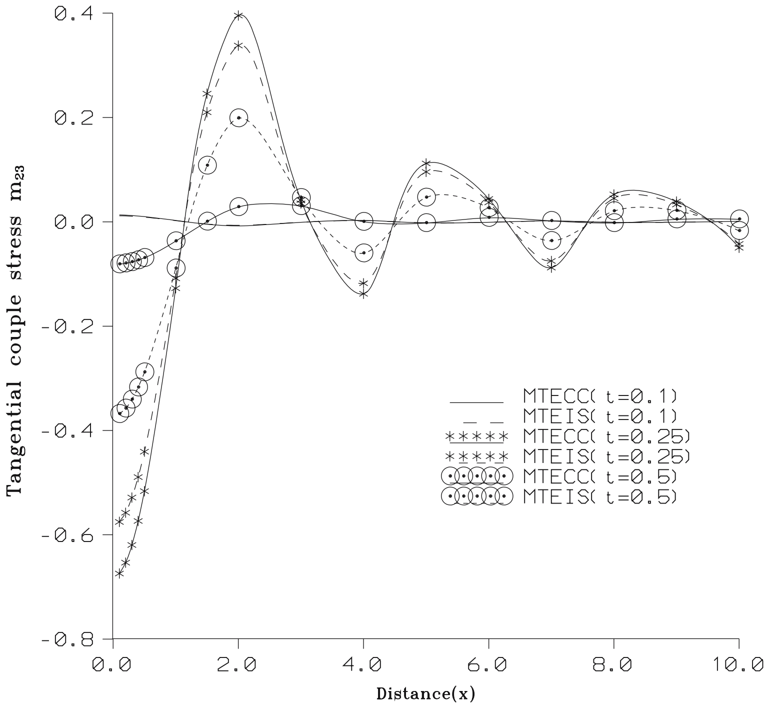

Fig. 2. Variation of tangential couple stress m_{23} with distance x (concentrated normal force: insulated boundary).

micropolar solid without energy dissipation possessing cubic symmetry as

$$\tilde{u}_1 = -\frac{1}{\Delta}\left[i\xi\left\{\Delta_1 \exp(-q_1 y) + \Delta_2 \exp(-q_2 y)\right\} + q_3 \Delta_3 \exp(-q_3 y) + q_4 \Delta_4 \exp(-q_4 y)\right], \tag{27}$$

$$\tilde{u}_2 = -\frac{1}{\Delta}\left[q_1 \Delta_1 \exp(-q_1 y) + q_2 \Delta_2 \exp(-q_2 y) - i\xi\left\{\Delta_3 \exp(-q_3 y) + \Delta_4 \exp(-q_4 y)\right\}\right. \tag{28}$$

$$\tilde{\phi}_3 = \frac{1}{\Delta}\left[a_3^* \Delta_3 \exp(-q_3 y) + a_4^* \Delta_4 \exp(-q_4 y)\right], \tag{29}$$

$$\tilde{t}_{22} = \frac{1}{\Delta}\left[r_1 \Delta_1 \exp(-q_1 y) + r_2 \Delta_2 \exp(-q_2 y) + r_3 \Delta_3 \exp(-q_3 y) + r_4 \Delta_4 \exp(-q_4 y)\right], \tag{30}$$

$$\tilde{t}_{21} = \frac{1}{\Delta}\left[s_1 \Delta_1 \exp(-q_1 y) + s_2 \Delta_2 \exp(-q_2 y) + s_3 \Delta_3 \exp(-q_3 y) + s_4 \Delta_4 \exp(-q_4 y)\right], \tag{31}$$

$$\tilde{m}_{23} = -\frac{B_3}{l^2 \rho c_1^2 \Delta}\left[a_3^* q_3 \Delta_3 \exp(-q_3 y) + a_4^* q_4 \Delta_4 \exp(-q_4 y)\right], \tag{32}$$

$$\tilde{T} = \frac{1}{\Delta}\left[a_1^* \Delta_1 \exp(-q_1 y) + a_2^* \Delta_2 \exp(-q_2 y)\right], \tag{33}$$

where

$$\begin{aligned}
\Delta &= f_1 f_2 - f_3 f_4, \quad f_1 = s_1 g_2^* - s_2 g_1^*, \quad f_2 = a_3^* q_3 r_4 - a_4^* q_4 r_3, \\
&\quad f_3 = r_1 g_2^* - r_2 g_1^*, \quad f_4 = a_3^* q_3 s_4 - a_4^* q_4 s_3, \\
\Delta_{1,2} &= \pm F f_4 g_{2,1}^* \tilde{\psi}_1(\xi), \quad \Delta_{3,4}^* = \pm F a_{4,3}^* q_{4,3} f_1 \tilde{\psi}_1(\xi), \\
g_{1,2}^* &= a_{1,2}^*\left(q_{1,2} - h\right), \quad r_n = -\xi^2 \frac{A_2}{\rho c_1^2} + q_n^2 - a_n^*, \\
r_\Theta &= -i\xi q_\Theta \left(1 - \frac{A_2}{\rho c_1^2}\right), \quad s_n = i\xi q_n \frac{(A_3 + A_4)}{\rho c_1^2}, \\
s_\Theta &= \frac{1}{\rho c_1^2}\left[A_3 q_\Theta^2 + \xi^2 A_4 + (A_3 - A_4) a_\Theta^*\right] \quad n = 1, 2; \quad \Theta = 3, 4.
\end{aligned} \tag{34}$$

3.1.1. *Concentrated Force*

In order to determine displacements, microrotation, stresses, and temperature due to the concentrated force described as a Dirac delta function, we use $\psi_1(x) = \delta(x)$ with

$$\tilde{\psi}_1(\xi) = 1. \tag{35}$$

3.1.2. *Uniformly Distributed Force*

The solution due to a uniformly distributed force applied on the half-space is obtained by setting

$$\psi_1(x) = \begin{bmatrix} 1 & \text{if} & |x| \le a, \\ 0 & \text{if} & |x| > a, \end{bmatrix}$$

in Eq. (26). The Fourier transform with respect to the pair (x, ξ) for the case of a uniform strip load of unit amplitude and width $2a$ applied at the plane boundary $y = 0$ in dimensionless form after suppressing the primes becomes

$$\tilde{\psi}_1(\xi) = [2 \sin(\xi a l)/\xi], \quad \xi \ne 0. \tag{36}$$

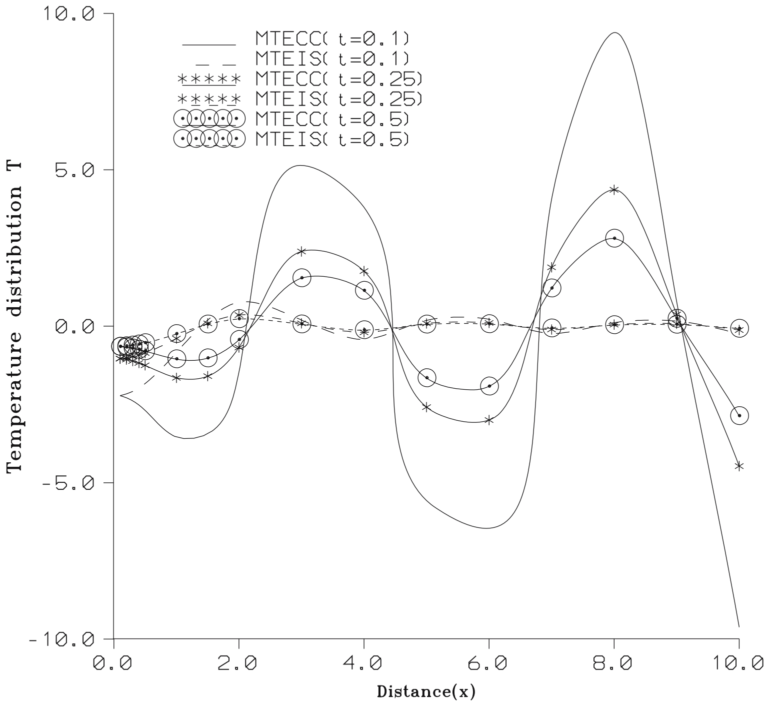

Fig. 3. Variation of temperature distribution T with distance x (concentrated normal force: insulated boundary).

3.1.3. Linearly Distributed Force

The solution due to a linearly distributed force is obtained by substituting

$$\psi_1(x) = \begin{bmatrix} 1 - \frac{|x|}{a} & \text{if} \quad |x| \le a, \\ 0 & \text{if} \quad |x| > a, \end{bmatrix}$$

in Eq. (26) where $2a$ is the width of the strip load. The Fourier transform for the case of a linearly distributed force applied at the plane boundary $y = 0$ of the Cartesian system, in dimensionless form is

$$\tilde{\psi}_1(\xi) = \frac{2\,[1 - \cos(\xi\, al)]}{\xi^2 al}\,. \tag{37}$$

The expressions for displacements, stresses, and temperature can be obtained for a concentrated force, a uniformly distributed force, and a linearly

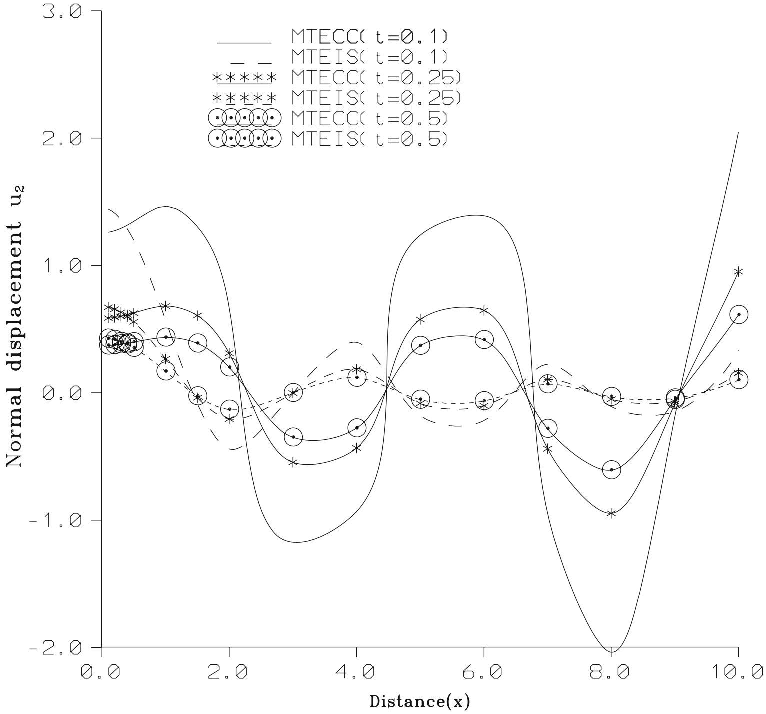

Fig. 4. Variation of normal displacement u_2 with distance x (uniformly distributed normal force: insulated boundary).

distributed force by replacing $\tilde{\psi}_1(\xi)$ from Eqs. (35)–(37), respectively, in Eqs. (27)–(33).

3.2. Thermoelastic Interactions due to Thermal Source

The boundary conditions in this case are

$$t_{22}=0,\quad t_{21}=0,\quad m_{23}=0,\quad \frac{\partial T}{\partial y}=r(x,t), \text{ for temperature gradient boundary}$$
$$\text{or} \tag{38}$$
$$T(x, y=0)=r(x,t), \text{ for temperature input boundary}$$

where $r(x,t)=\eta(x)\delta(t)$.

Applying Laplace and Fourier transforms defined by Eqs. (15) and (16) on Eq. (38), we get

$$r(\xi, p)=\tilde{\eta}(\xi).$$

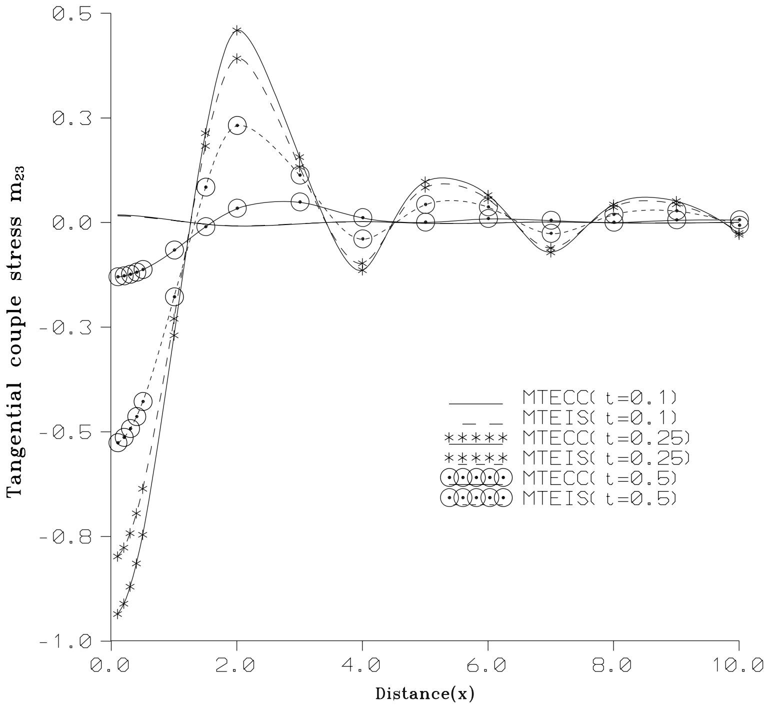

Fig. 5. Variation of tangential couple stress m_{23} with distance x (uniformly distributed normal force: insulated boundary).

The expressions for displacement, force stress, tangential couple stress, and temperature distribution are given by Eqs. (27)–(33) with Δ_υ replaced by Δ_υ^0 $(\upsilon = 1, 2, 3, 4)$ in Eq. (34) where

$$\begin{aligned} \Delta_{1,2}^0 &= \mp H\tilde{\eta}(\xi)\left[-a_3^* q_3 \left(r_{2,1}s_4 - r_4 s_{2,1}\right) + a_4^* q_4 \left(r_{2,1}s_3 - r_3 s_{2,1}\right)\right], \\ \Delta_{3,4}^0 &= \mp H\,\tilde{\eta}(\xi)\, a_{4,3}^* q_{4,3} \left(r_1 s_2 - r_2 s_1\right). \end{aligned} \tag{39}$$

and $H = \frac{l}{T_0}$ for a temperature gradient boundary and $H = \frac{1}{T_0}$ for a temperature input boundary.

3.2.1. Thermal Point Source

For this case

$$\eta(x) = \delta(x)$$

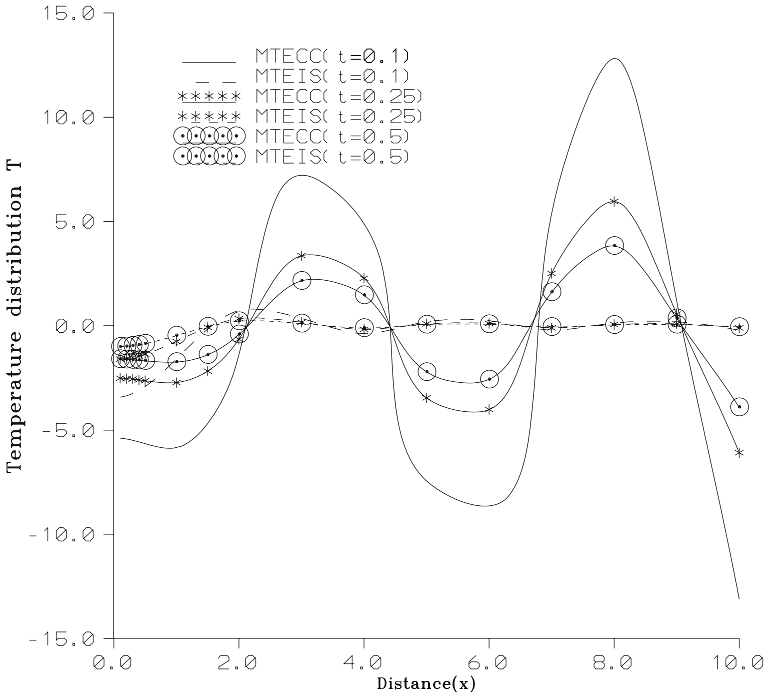

Fig. 6. Variation of temperature distribution T with distance x (uniformly distributed normal force: insulated boundary).

with

$$\tilde{\eta}(\xi) = 1. \tag{40}$$

3.2.2. Uniformly Distributed Thermal Source

For this case

$$\eta(x) = \begin{bmatrix} 1 & \text{if} & |x| \leq a, \\ 0 & \text{if} & |x| > a, \end{bmatrix}$$

with

$$\tilde{\eta}(\xi) = [2 \sin(\xi a l)/\xi], \quad \xi \neq 0. \tag{41}$$

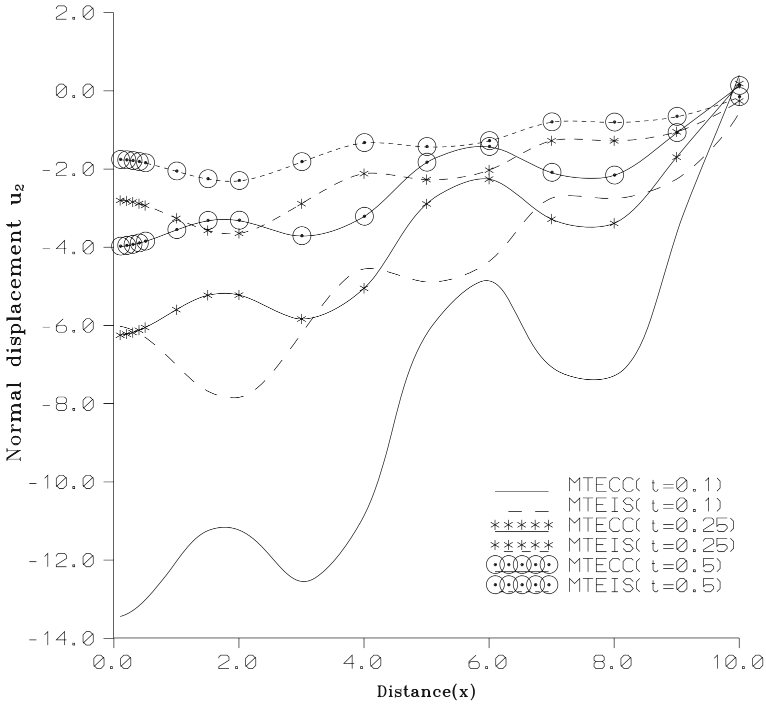

Fig. 7. Variation of normal displacement u_2 with distance x (linearly distributed normal force: insulated boundary).

3.2.3. Linearly Distributed Thermal Source

For this case

$$\eta(x) = \begin{bmatrix} 1 - \frac{|x|}{a} & \text{if} \quad |x| \le a, \\ 0 \quad \text{if} \quad |x| > a, \end{bmatrix}$$

with

$$\tilde{\eta}(\xi) = \frac{2\,[1 - \cos(\xi\, al)]}{\xi^2 al}\,. \tag{42}$$

The expressions for the components of displacement, microrotation, force stress, couple stress, and temperature can be obtained for a thermal point source, a uniformly distributed thermal source, and a linearly distributed thermal source by replacing $\tilde{\eta}(\xi)$ from Eqs. (40)–(42), respectively, in Eqs. (27)–(33).

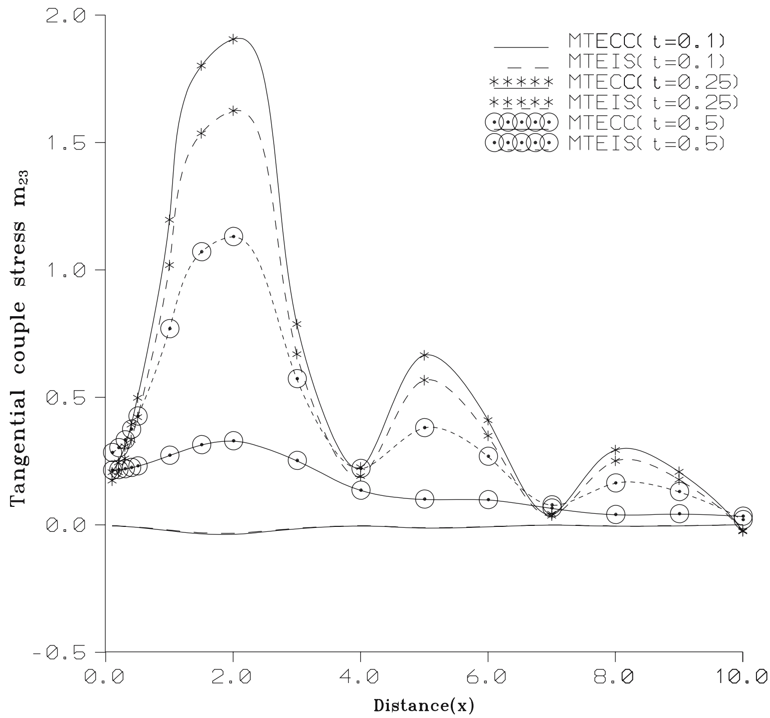

Fig. 8. Variation of tangential couple stress m_{23} with distance x (linearly distributed normal force: insulated boundary).

4. PARTICULAR CASES

Case A—Neglecting the micropolarity effect (i.e.,$B_3 = j = 0$) in Eqs. (27)–(33), we obtain the corresponding expressions for the components of displacement, force stress, couple stress, and temperature distribution in a thermoelastic medium possessing cubic symmetry. The expressions for the components of displacement, force stress, couple stress, and temperature distribution can be obtained for a concentrated force, a uniformly distributed force, and a linearly distributed force by replacing $\tilde{\psi}_1(\xi)$ from Eqs. (35)–(37), respectively, in Eqs. (27)–(33) after neglecting the micropolarity effect.

Case B—Neglecting the thermal effect in Eqs. (27)–(33), the expressions for the components of displacements, microrotation, force stress, and couple stress are obtained in a micropolar medium possessing cubic symmetry. Again the expressions for the components of displacement, microrotation, force stress, and couple stress can be obtained for a concentrated

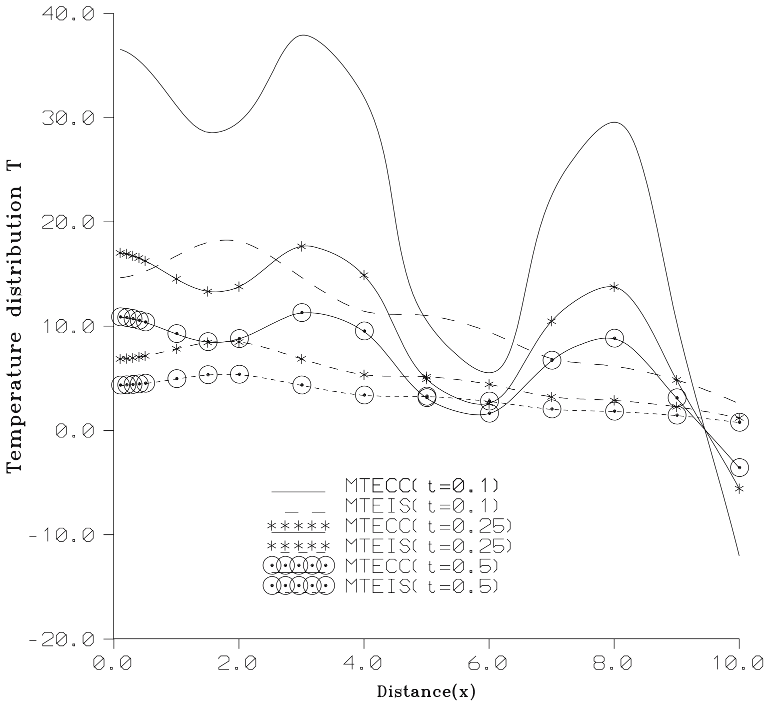

Fig. 9. Variation of temperature distribution T with distance x (linearly distributed normal force: insulated boundary).

force, a uniformly distributed force, and a linearly distributed force by replacing $\tilde{\psi}_1(\xi)$ from Eqs. (35)–(37), respectively, in Eqs. (27)–(33) after neglecting the thermal effect.

4.1. Thermoelastic Micropolar Solid

(A) Taking $A_1 = \lambda + 2\mu + K, \quad A_2 = \lambda, \quad A_3 = \mu + K, \quad A_4 = \mu, \quad B_3 = \gamma$ (43)

in Eqs. (27)–(33) with Eqs. (35)–(37), we obtain the corresponding expressions in for an isotropic thermoelastic micropolar medium, an isotropic thermoelastic medium (on neglecting micropolarity effect), and an isotropic micropolar medium (on neglecting thermal effect) for a concentrated force, a uniformly distributed force, and a linearly distributed force, respectively.

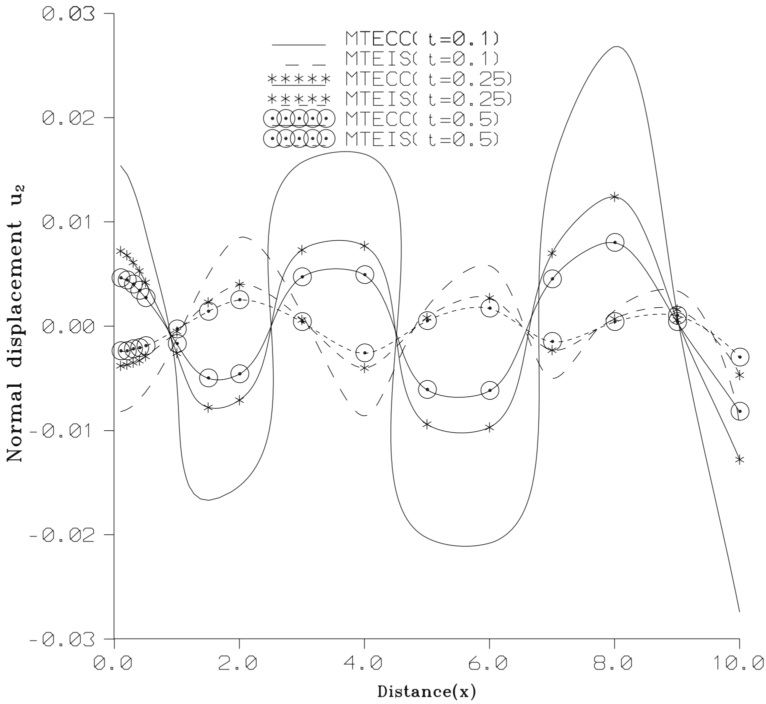

Fig. 10. Variation of normal displacement u_2 with distance x (thermal point source: insulated boundary).

(B) Using Eq. (43) in Eqs. (27)–(33) with Δ_υ replaced by $\Delta_\upsilon^0 (\upsilon = 1, 2, 3, 4)$ from Eq. (39) and using Eqs. (42)–(44), we obtain the corresponding expressions for a thermal source, a uniformly distributed thermal source, and a linearly distributed thermal source, respectively.

Sub case 1—If $h \to 0$, Eqs. (27)–(33) yields the expressions for displacements, microrotation, force stress, couple stress, and temperature distribution for an insulated boundary. For this case, $H = \frac{l}{T_0}$ in Eq. (39).

Sub case 2—If $h \to \infty$, Eqs. (27)–(33) yields the expressions for displacements, microrotation, force stress, couple stress, and temperature distribution for an isothermal boundary. For this case, $H = \frac{1}{T_0}$ in Eq. (39).

5. INVERSION OF THE TRANSFORM

The transformed displacements and stresses are functions of y and the parameters of Laplace and Fourier transforms p and ξ, respectively, and hence are of the form $\tilde{f}(\xi, y, p)$. To get the function in the physical

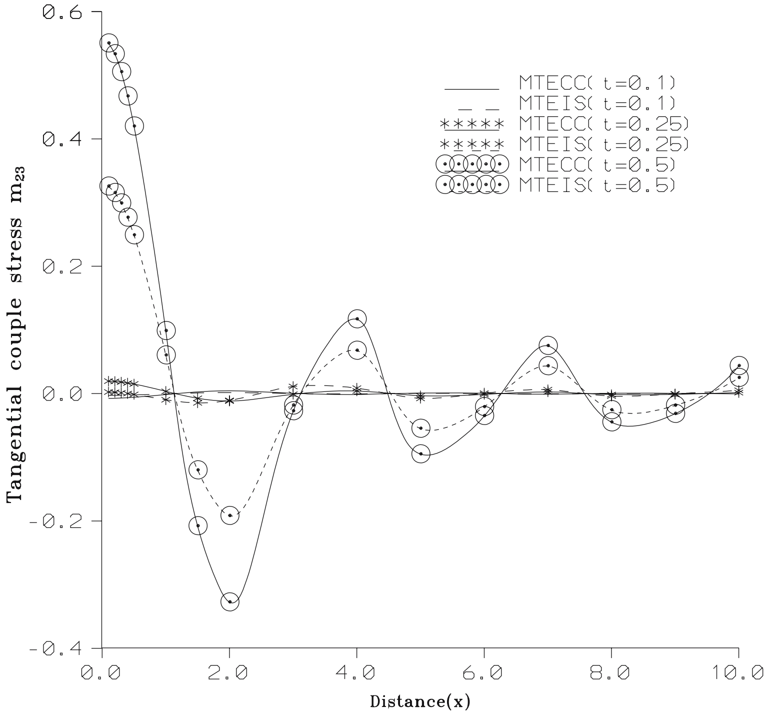

Fig. 11. Variation of tangential couple stress m_{23} with distance x (thermal point source: insulated boundary).

domain, we invert the Fourier and Laplace transforms using the method already discussed by Kumar and Ailawalia [19].

6. NUMERICAL RESULTS AND DISCUSSIONS:

For numerical computations, we take the following values of relevant parameters for micropolar medium possessing cubic symmetry as $A_3 = 5.6 \times 10^{10}\,\mathrm{N \cdot m^{-2}}$, $A_2 = 11.7 \times 10^{10}\ \mathrm{N \cdot m^{-2}}$, $A_4 = 4.3 \times 10^{10}\ \mathrm{N \cdot m^{-2}}$, $B_3 = 0.98 \times 10^{-9}\ \mathrm{N}$.

For comparison with a micropolar isotropic solid, following Eringen [21] and Dhaliwal and Singh [22], we take the following values of relevant parameters for the case of a magnesium crystal-like material as $\rho = 1.74 \times 10^3\mathrm{kg\,m^{-3}}$, $\lambda = 9.4 \times 10^{10}\,\mathrm{N \cdot m^{-2}}$, $\mu = 4.0 \times 10^{10}\,\mathrm{N \cdot m^{-2}}$; $K = 1.0 \times 10^{10}\,\mathrm{N \cdot m^{-2}}$, $\gamma = 0.779 \times 10^{-9}\ \mathrm{N}$, $j = 0.2 \times 10^{-19}\ \mathrm{m^2}$; $C^* = 0.4353 \times 10^{10}\,\mathrm{J\,kg^{-1}\,{}^\circ C^{-1}}$, $\nu = 0.0268 \times 10^8\,\mathrm{N \cdot m^{-2}\,{}^\circ C^{-1}}$, $T_0 = 23\,{}^\circ\mathrm{C}$; $K^* = 1.7 \times 10^4\ \mathrm{J\,s^{-1}\,m^{-2}\,{}^\circ C^{-1}}$, $F = 1.0$. The values of the normal displacement u_2, the

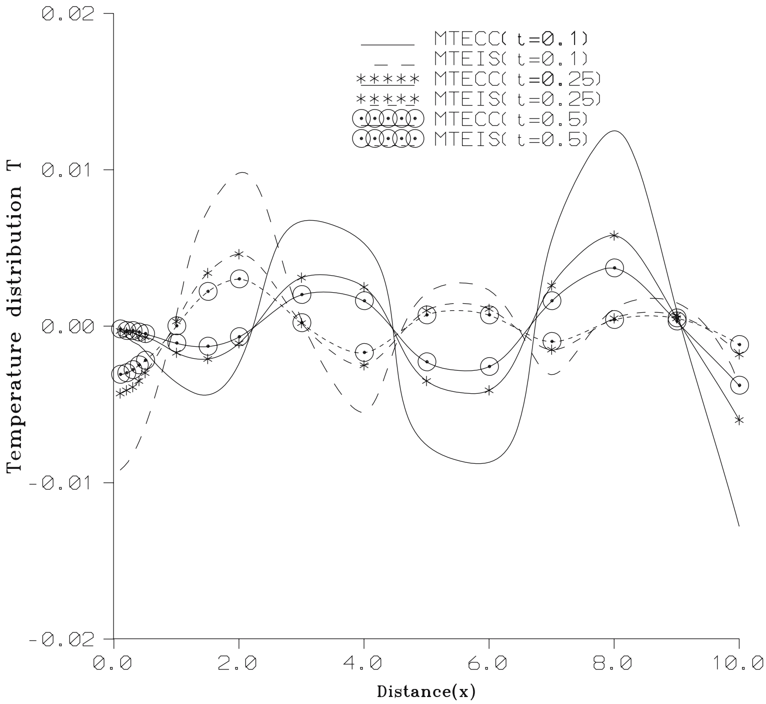

Fig. 12. Variation of temperature distribution T with distance x (thermal point source: insulated boundary).

tangential couple stress m_{23}, and the temperature distribution T for a thermoelastic micropolar solid with cubic symmetry (MTECC) and a thermoelastic micropolar isotropic solid (MTEIS) have been studied for a normal force and insulated boundary at $t = 0.1$, 0.25, and 0.5. The variations of these components with distance x have been shown by (a) solid line (———) for MTECC and dashed line (--------) for MTEIS at $t = 0.1$, (b) solid line with centered symbol (∗—∗—∗) for MTECC and dashed line with centered symbol (∗---∗---∗) for MTEIS at $t = 0.25$, and (c) solid line with centered symbol (⊙—⊙—⊙) for MTECC and dashed line with centered symbol (⊙---⊙---⊙) for MTEIS at $t = 0.5$. These variations are shown in Figs. 1–18. The comparison between a thermoelastic micropolar cubic crystal and a thermoelastic micropolar isotropic solid is shown. All the results are for one value of dimensionless width, $a = 1.0$. The computations are carried out for $y = 1.0$ and $l = 1.0$, cm in the range $0 \leq x \leq 10.0$.

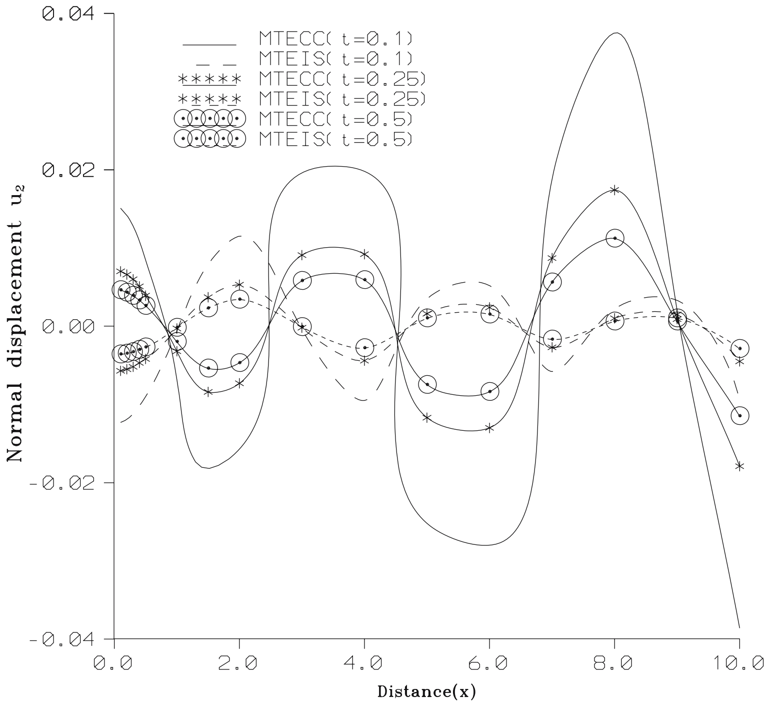

Fig. 13. Variation of normal displacement u_2 with distance x (uniformly distributed thermal source: insulated boundary).

7. DISCUSSIONS FOR VARIOUS CASES

7.1. Mechanical Forces

7.1.1. Concentrated Force

At any particular time, the values of the normal displacement are smaller for MTEIS as compared to the values for MTECC. Also, the magnitudes of oscillations of the normal displacement decrease with an increase in time. These variations of the normal displacement are shown in Fig. 1.

The variations of the tangential couple stress are oscillatory in nature for both MTECC and MTEIS. These oscillations are smoother in nature as compared to the oscillations obtained for normal displacement. Also, the magnitudes of these oscillations decrease with an increase in the horizontal distance. Very near to the time of application of the source (at $t=0.1$), the values of the tangential couple stress are smaller in comparison

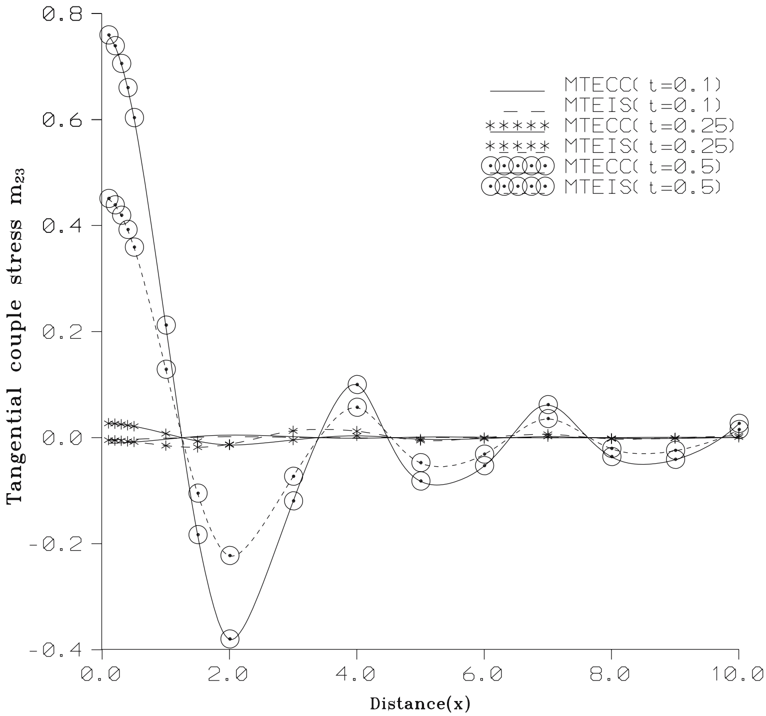

Fig. 14. Variation of tangential couple stress m_{23} with distance x. (uniformly distributed thermal source: insulated boundary).

to the values obtained at other intervals of time. These variations of the tangential couple stress are shown in Fig. 2.

It is observed from Fig. 3 that the values of the temperature distribution for MTEIS lie in a very short range, so these variations for MTEIS are comparable to the variations obtained for the case of normal displacement but the variations of the temperature distribution for MTECC are opposite in nature to the variations of the normal displacement.

7.1.2. Uniformly Distributed Force

The variations of all the quantities, i.e., the normal displacement, the tangential couple stress, and the temperature distribution for the case of a uniformly distributed force are very similar to the variations obtained for these quantities for the case of a concentrated force. Although the variations of the quantities and their discussions are the same, the difference in magnitude for both cases is significant. These variations of the normal

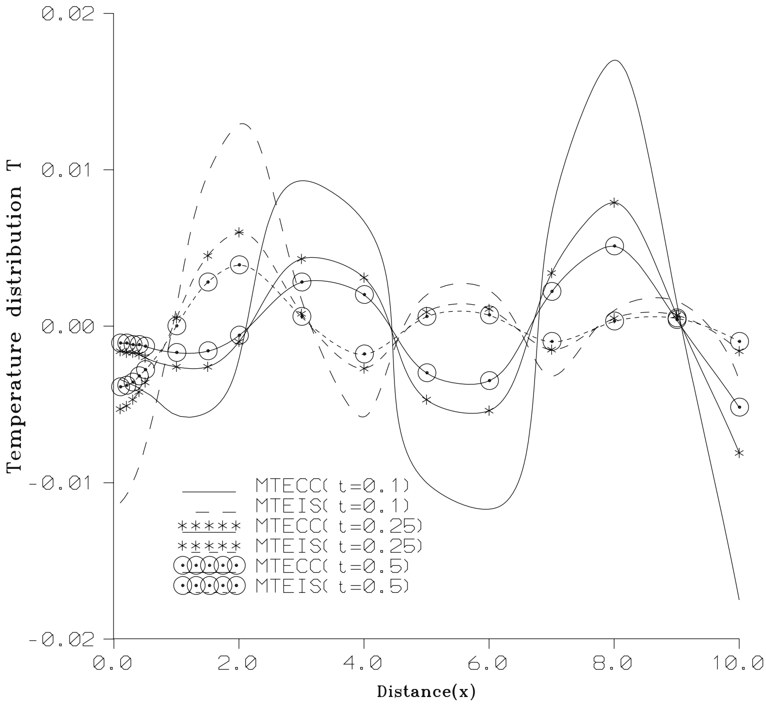

Fig. 15. Variation of temperature distribution T with distance x (uniformly distributed thermal source: insulated boundary).

displacement, the tangential couple stress, and the temperature distribution for a uniformly distributed force are shown in Figs. 4–6, respectively.

7.1.3. Linearly Distributed Force

On application of a linearly distributed force, the variations of the normal displacement being oscillatory in nature follow an increasing trend with an increase in horizontal distance. The degree of the increase in magnitude, however, decreases with an increase in time. Also, very close to the point of application of the source, the values of the normal displacement for both MTECC and MTEIS increase with an increase in time. At a particular time, the magnitude of the normal displacement for MTEIS is less compared to the value for MTECC. These variations of the normal displacement are shown in Fig. 7.

As discussed for the case of a concentrated force and a uniformly distributed force, the values of the tangential couple stress for both MTECC and MTEIS at $t = 0.1$ lie in a very short range. However, the variations

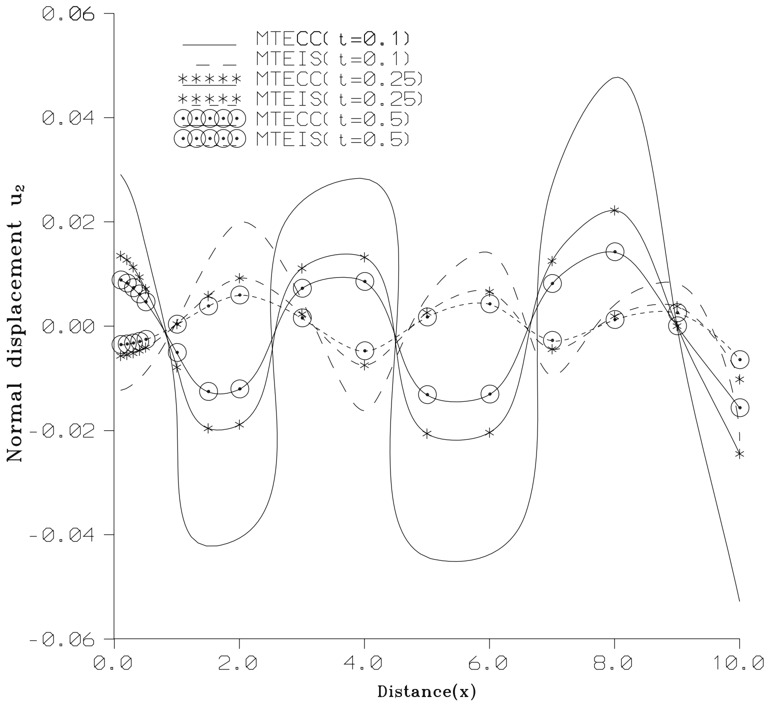

Fig. 16. Variation of normal displacement u_2 with distance x (linearly distributed thermal source: insulated boundary).

obtained at $t = 0.25$ and $t = 0.5$ are opposite in nature to the variations obtained in the previous two cases at the same times. These variations of the tangential couple stress are shown in Fig. 8.

As observed from Fig. 9, the variations of the temperature distribution are opposite in nature to the variations of the normal displacement. Hence, the values of the temperature distribution, close to the point of application of the source, decrease with an increase in distance x. Also, the values of the temperature distribution for MTEIS are less in comparison to the values for MTECC.

7.2. Thermoelastic Interactions due to Thermal Sources

7.2.1. Thermal Source

The variations of all the quantities are opposite in nature to the variations obtained for the case of a concentrated force. Although the

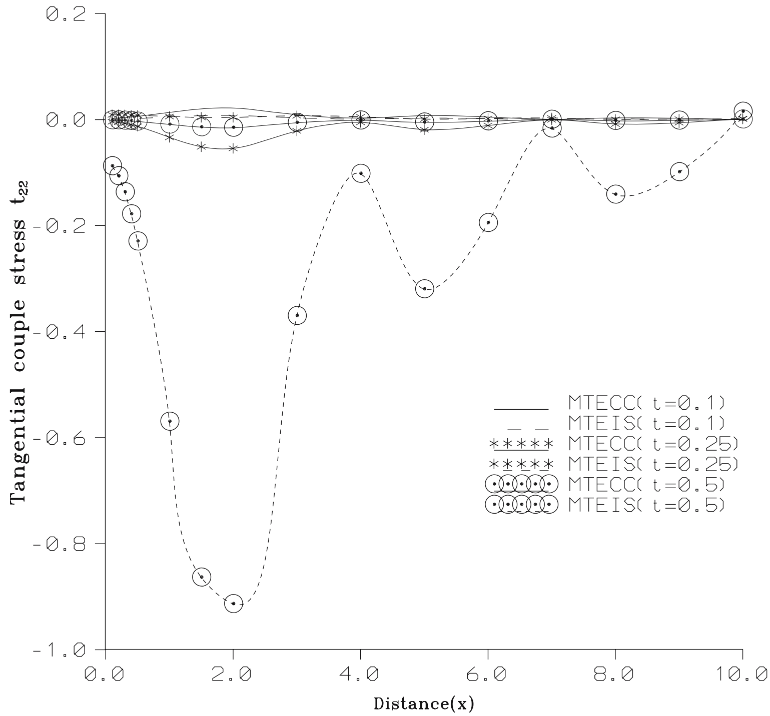

Fig. 17. Variation of tangential couple stress m_{23} with distance x (linearly distributed thermal source: insulated boundary).

difference between the values is quite significant, it is important to note that the values obtained for the case of a thermal point source are much less in comparison to the values obtained for the case of a mechanical load. The variations of the normal displacement, the tangential couple stress, and the temperature distribution are shown in Figs. 10–12, respectively.

7.2.2. Uniformly Distributed Thermal Source

The variations of the normal displacement and tangential couple stress are opposite in nature to the variations obtained for the case of a uniformly distributed force. These variations of the normal displacement, the tangential couple stress, and the temperature distribution on application of a uniformly distributed thermal source are shown in Figs. 13–15, respectively.

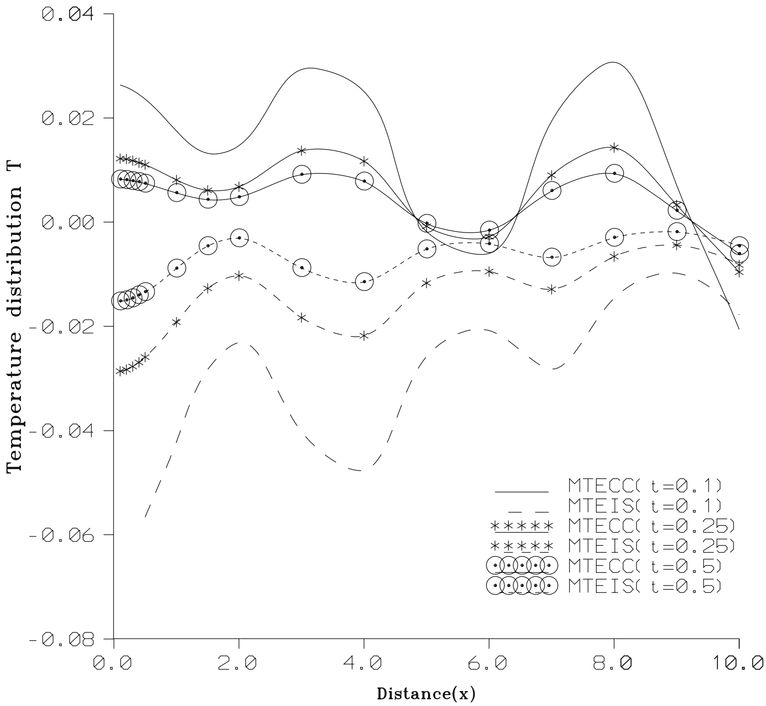

Fig. 18. Variation of temperature distribution T with distance x (linearly distributed thermal source: insulated boundary).

7.3. Linearly Distributed Thermal Source

For MTECC the variations of the temperature distribution for this case are very similar in nature with the variations of the temperature distribution obtained for the case of a linearly distributed force (mechanical). But the variation of these quantities for MTEIS are more oscillatory in nature as compared to the variations for a linearly distributed force. Also, the magnitudes of these oscillations decrease with an increase in time. The variations of the normal displacement and tangential couple stress for both MTECC and MTEIS are similar to the variations obtained for the case of a uniformly distributed thermal source with a difference in magnitude. The variations of the normal displacement, the tangential couple stress, and the temperature distribution are shown in Figs. 16–18, respectively.

8. CONCLUSION

The properties of a body depend largely on the direction of symmetry. The variations of all the quantities are similar in nature on the application of a concentrated mechanical force and a uniformly distributed force with a difference in magnitude. The body is deformed to a much more extent on the application of a mechanical source, since the values of all the quantities obtained for the case of a thermal source are much less.

REFERENCES

1. H. W. Lord and Y. Shulman, *J. Mech. Phys. Solids* **15**:299 (1967).
2. A. E. Green and K. A. Lindsay, *J. Elasticity* **2**:1 (1972).
3. A. E. Green and P. M. Naghdi, *J. Elasticity* **31**:189 (1993).
4. A. C. Eringen, *J. Math. Mech.* **15**:909 (1966).
5. R. Kumar and S. Choudhary, *Arch. Mech.* **54**:185 (2002).
6. R. Kumar and S. Choudhary, *J. Vibration and Control* **8**:1053 (2002).
7. R. Kumar and S. Choudhary, *Meccanica* **38**:349 (2003).
8. D. H. Chung and W. R. Buessem, *J. Appl. Phys.* **38**:2010 (1967).
9. K.-H. C. Lie and J. S. Koehler, *Adv. Phys*. **17**:421 (1968).
10. J. W. Steeds, *Introduction to Anisotropic Elasticity Theory of Dislocations* (Clarendon Press, Oxford, 1973).
11. P. Boulanger and M. Hayes, *Z. Angew. Math. Phys.* **51**:1031 (2000).
12. A. Bertram, T. Bohlke, N. Gaffke, B. Heiligers, and R. Offinger, *J. Elasticity* **58**:233 (2000).
13. R. Kobayashi and Y. Giga, *Jpn. J. Indust. Appl. Math.* **18**:207 (2001).
14. W. Domanski and T. Jablonski, *Arch. Mech.* **53**:91 (2001).
15. M. Destrade, *J. Acous. Soc. Am.* **109**:1398 (2001).
16. F. Zhou and A. Ogawa, *ASME J. Appl. Mech.* **69**:81 (2002).
17. S. Minagawa, K. Arakawa, and M. Yamada, *Bull. JSME* **24**:22 (1981).
18. R. Kumar and L. Rani, *Int. J. Appl. Mech. Eng.* **8**:637 (2003).
19. R. Kumar and P. Ailawalia, *J. Sound Vibration* **283**:875 (2005).
20. R. Kumar and P. Ailawalia, *Int. J. Solids Structures* **42**:5931 (2005).
21. A. C. Eringen, *Int. J. Eng. Sci*. **22**:1131 (1984).
22. R. S. Dhaliwal and A. Singh, *Dynamic Coupled Thermoelasticity* (Hindustan Pub. Corp., New Delhi, India, 1980), p. 276.